Numerical investigation of the lateral–torsional buckling of beams with slender cross sections for the case of fire

Carlos Couto [a], Paulo Vila Real [a,*], Nuno Lopes [a], Bin Zhao [b]

[a] RISCO – Civil Engineering Department, University of Aveiro, Campus Universitário de Santiago, 3810-193 Aveiro, Portugal
[b] CTICM – Centre Technique Industriel de la Construction Métallique, Parc Technologique L'Orme des Merisiers – Immeuble Apollo, 91193 Saint Aubin, Paris, France

ABSTRACT

An extensive numerical study is performed to investigate the lateral–torsional buckling of steel beams with slender cross sections for the case of fire. The influence of local buckling is analysed, and the numerical results are compared to the simplified design methods of Part 1-2 of Eurocode 3 for the case of beams with Class 1 and 2 cross sections. The actual provisions of Eurocode 3 Part 1-2 are demonstrated to be unreliable. A parametric study is carried out to investigate the influence of several parameters on the resistance of laterally unrestrained steel beams with slender cross sections for the case of fire: the effective section factor, temperature, steel grade, depth-to-width ratio (h/b) and residual stresses. Based on the parametric study, a proposal for a new design curve is made for beams with slender cross sections for the case of fire, taking into account the influence of local buckling by grouping the response of beams into different ranges of effective section factors. The capacity predicted by the simplified methods using the proposed design curve leads to an improved yet safe design method compared to the results of the finite element analysis.

© 2015 Elsevier Ltd. All rights reserved.

1. Introduction

This paper addresses the lateral–torsional buckling (LTB) behaviour of laterally unrestrained steel beams with slender cross sections for the case of fire. Slender cross sections are composed of plates with a high width-to-thickness ratio (slenderness) and, for that reason, are prone to local buckling. Studies about the influence of local buckling in LTB are very scarce for fire situations because LTB has been mainly studied for beams with cross sections without local buckling instability. Bailey et al. [1] numerically investigated the LTB of unrestrained steel beams and concluded that both British code and the Eurocode, at that time, overestimated the limiting temperatures for unrestrained simple beams in fire resistance calculations. Vila Real and Franssen [2] performed a numerical study and proposed a design curve for the LTB of steel beams. This design curve was later adopted in the final version of the Eurocode 3 Part 1-2 (EN 1993-1-2) [3]. The experimental investigation conducted by Vila Real et al. [4], and later by Mesquita et al. [5], carried out on the LTB of steel beams at elevated temperatures was used to validate the proposed method by Vila Real and Franssen [2]. Vila Real et al. [6,7] also studied the influence of the residual stresses

in the LTB of steel beams and concluded that for Class 1 members, the residual stresses are negligible, subsequently widening the initial proposal to account for other loading types. An improved proposal for the lateral–torsional buckling of unrestrained steel beams subjected to elevated temperatures was later presented by Vila Real et al. [8]. In this publication, the influence of loading type, steel grade, pattern of the residual stresses (hot-rolled or welded sections) and the h/b ratio, i.e., the depth h and the width b of the cross section, on the resistance of the beam was addressed through an extensive numerical study. Based on this study, a proposal to include a factor to account for other loading cases (the factor "f") as well as a severity factor for the influence of the steel grade in the current design method of Part 1-2 was presented. Dharma and Tan [9] proposed two alternative approaches to the current design method of Eurocode 3 Part 1-2 based on numerical investigation to calculate the lateral–torsional buckling resistance for the case of fire. They proposed an alternative approach to address the discontinuity between the design method at high temperature and at room temperature, an approach based on the Rankine formula that enables the failure temperature to be determined directly, without an iterative procedure, as required in the EN 1993-1-2 design method. In these studies, the beams were considered uniformly heated, and the influence of other temperature distributions was not addressed. On this subject, Yin and Wang [10] have numerically investigated the effects of several design factors

---

* Corresponding author. Tel.: +351 234370049; fax: +351 234370094.
 E-mail address: pvreal@ua.pt (P. Vila Real).

on the lateral–torsional buckling bending moment resistance of steel I-beams submitted to non-uniform temperature distributions. A proposal was made for a modification to the lateral–torsional buckling slenderness of the beam to account for the non-uniform distribution of the temperature along the cross section; however, only the variation of the temperature in the depth of the cross section was considered. Later, Zhang et al. [11] analysed the LTB behaviour of beams subjected to localised fires and concluded that the failure temperature may be considerably lower than that of uniformly heated beams. Further investigation on the LTB resistance on non-uniformly heated beams should be performed but is outside of the scope of the present study. More recently, a numerical investigation by Lopes and Vila Real [12] on Class 4 stainless steel beams was performed. The influence of the geometrical imperfections (local, global and both) and the residual stresses was analysed at high temperatures, and it was concluded that they are relevant for determining the ultimate load and therefore should be considered according to the expected collapse mode.

Apart from [12], which consists of a study of stainless steel members, none of the remaining studies address slender cross sections prone to local buckling and the influence of local buckling on the LTB resistance of beams. Eurocode 3 [13] classifies these cross sections where local buckling prevents the yield strength from being reached in the compressed parts of the cross sections as Class 4, the highest class. Furthermore, in the establishment of the design rules of Eurocode 3 [3] for the case of fire (Part 1-2), the simple design methods were assumed to be adequate for designing beams with Class 4 cross sections if the recommendations of Annex E of that standard were followed. Annex E of Part 1-2 of the Eurocode 3 suggests the use of an effective cross section determined for normal temperature and the use of 0.2% proof strength ($f_{0.2p,\theta}$, see Fig. 1) for the design yield strength. Thus, the influence of local buckling is accounted for by reducing the cross-sectional capacity, by reducing the effective area, and by considering a reduced value of the yield strength.

The recommendations of Annex E are essentially based on the early work of Ranby [15], who studied Class 4 plates at elevated temperatures. On this matter, the authors [16–18] reached the same conclusions for cross sections that are built up exclusively of plates classified as Class 4 but demonstrated that for Class 4 cross sections with non-Class 4 plates, these recommendations lead to inaccurate results. Local buckling was also shown to prevent the elastic bending resistance being reached even in Class 3 cross sections. Thus, the load bearing capacity of the members with such cross sections is affected and needs to be investigated.

At ambient temperature, investigation on steel members with slender cross sections where failure may occur in a complex local–global interaction has also drawn the attention of different researchers. The "Direct Strength Method" (DSM) developed by Schafer and Pekoz [19] reviewed by Schafer [20] is based on determining the strength of a structural component as an explicit function of its gross cross-sectional properties, elastic critical buckling stresses for all relevant instability modes (i.e., global buckling, local buckling and distortional buckling) and yield strength, without the need to define an effective cross-section. The "Erosion of Critical Buckling Load" (ECBL) approach developed by Dubina [21], of which a review is given by Dubina and Ungureanu in [22], enables the numerical evaluation of the theoretical erosion of critical load into the interactive buckling range. The procedure can be used to calibrate the imperfection factor used to check the buckling strength of members as defined in Eurocode 3. Camotim et al. [23], who used the Generalised Beam Theory (GBT) to analyse the buckling behaviour of steel beams with several loadings and support conditions (including intermediate supports) have presented in [24] their current developments towards an efficient direct approach to estimate the ultimate loading of continuous beams, which may fail in complex modes that combine local, distortional and global features.

In this paper, an extensive numerical investigation is performed by finite element analysis (FEA) to study the influence of local buckling on the LTB resistance of beams with Class 3 and Class 4 cross sections under fire conditions. The effect of temperature, residual stresses, steel grade and the depth-to-width ratio (h/b) on the LTB resistance of beams with slender cross sections are also detailed. Using new methodology to calculate the cross section resistance developed by the authors [16–18] together with the Eurocode 3 Part 1-2 beam design curve leads to an improvement on the results compared to FEA calculations. However, this design curve should be slightly changed for Class 3 and Class 4 cross sections, and a proposal for a new design curve is made. Accordingly, an effective section factor is proposed to group the behaviour of beams with slender cross sections in a way that the interaction between local and lateral–torsional buckling may be accounted
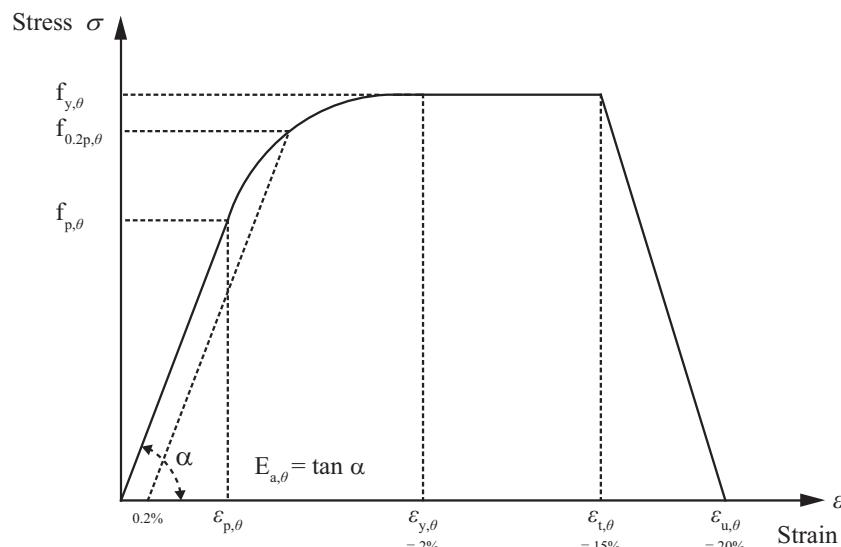

Fig. 1. Stress–strain relationship for carbon steel at elevated temperatures [14].

for in the case of fire. With this, better agreement between the simplified design methods and the numerical results is achieved, leading to an improved yet safe design method.

2. Lateral–torsional buckling of beams with Class 3 and 4 cross sections at elevated temperatures

2.1. Eurocode 3 Part 1-2

According to Part 1-2 of the Eurocode 3, the resistance of laterally unrestrained beams in bending at elevated temperature ($M_{b,fi,t,Rd}$) should be verified according to Eq. (1) for members with Class 3 cross sections and according to Eq. (2) for Class 4 cross sections.

$$M_{b,fi,t,Rd} = \chi_{LT,fi} W_{el,y} k_{y,\theta} f_y / \gamma_{M,fi} \tag{1}$$

$$M_{b,fi,t,Rd} = \chi_{LT,fi} W_{eff,min,y} k_{0.2p,\theta} f_y / \gamma_{M,fi} \tag{2}$$

where $W_{el,y}$ is the elastic section modulus, $W_{eff,y,min}$ is the section modulus of the effective cross section calculated with the same rules as for normal temperature, $k_{y,\theta}$ and $k_{0.2p,\theta}$ are the reduction factors for the effective yield strength and the design strength of Class 4 cross sections both relative to f_y, and f_y is the design yield strength and its respective safety factor for fire design situation is $\gamma_{M,fi}$. The difference between Eqs. (1) and (2) is the use of the effective section modulus ($W_{eff,y}$) and the steel 0.2% proof strength ($f_{0.2p,\theta} = k_{0.2p,\theta} f_y$) in Eq. (2), whereas in Eq. (1), the elastic section modulus of the gross cross section ($W_{el,y}$) and the yield strength ($f_{y,\theta} = k_{y,\theta} f_y$) are used. The reduction factor for LTB in the fire design situation is determined by

$$\chi_{LT,fi} = \frac{1}{\phi_{LT,\theta} + \sqrt{\phi_{LT,\theta}^2 - \bar{\lambda}_{LT,\theta}^2}} \tag{3}$$

and

$$\phi_{LT,\theta} = 0.5[1 + \alpha \bar{\lambda}_{LT,\theta} + \bar{\lambda}_{LT,\theta}^2] \tag{4}$$

with the imperfection factor given by

$$\alpha = 0.65\varepsilon = 0.65\sqrt{235/f_y} \tag{5}$$

with the non-dimensional slenderness at elevated temperatures given by Eq. (6) for Class 3 cross sections and Eq. (7) for Class 4 cross sections.

$$\bar{\lambda}_{LT,\theta} = \bar{\lambda}_{LT}\sqrt{k_{y,\theta}/k_{E,\theta}} \tag{6}$$

$$\bar{\lambda}_{LT,\theta} = \bar{\lambda}_{LT}\sqrt{k_{0.2p,\theta}/k_{E,\theta}} \tag{7}$$

with

$$\bar{\lambda}_{LT} = \sqrt{W_{y,min}f_y/M_{cr}} \tag{8}$$

where $W_{y,min}$ is the elastic section modulus $W_{el,y}$ for Class 3 cross sections or the effective section modulus $W_{eff,y,min}$ for Class 4 cross sections, $k_{E,\theta}$ is the reduction factor for the *Young's modulus* at elevated temperatures given in EN 1993-1-2, and M_{cr} is the elastic critical moment given in the literature, based on gross cross-sectional properties and taking into account the loading conditions, the real moment distribution and the lateral restraints.

2.2. Using a new methodology to calculate the cross-sectional resistance

According to the methodology developed by the authors in [17,18] to assess the cross-sectional resistance of Class 3 and Class 4 cross sections, Eq. (9) should be used to check the resistance of laterally unrestrained beams in bending at elevated temperatures. In this proposal, the reduction factor $k_{y,\theta}$ is used for Class 4 sections as for the other cross sections, instead of the reduction factor $k_{0.2p,\theta}$.

$$M_{b,fi,t,Rd} = \chi_{LT,fi} W_{new,eff,y} k_{y,\theta} f_y / \gamma_{M,fi} \tag{9}$$

with $\chi_{LT,fi}$ given in Eq. (3), but considering the non-dimensional slenderness at elevated temperatures as

$$\bar{\lambda}_{LT,\theta} = \bar{\lambda}_{LT}\sqrt{k_{y,\theta}/k_{E,\theta}} \tag{10}$$

The new effective section modulus, $W_{new,eff,y}$, is calculated with the same principles as for normal temperature but considering the plate reduction factors for internal compression elements as [9,10]:

$$\rho = \frac{\left(\bar{\lambda}_p + 0.9 - \frac{0.26}{\varepsilon}\right)^{1.5} - 0.055(3 + \psi)}{\left(\bar{\lambda}_p + 0.9 - \frac{0.26}{\varepsilon}\right)^3} \leqslant 1.0 \tag{11}$$

and for outstand compression elements as [17,18]:

$$\rho = \frac{\left(\bar{\lambda}_p + 1.1 - \frac{0.52}{\varepsilon}\right)^{1.2} - 0.188}{\left(\bar{\lambda}_p + 1.1 - \frac{0.52}{\varepsilon}\right)^{2.4}} \leqslant 1.0 \tag{12}$$

with $\varepsilon = \sqrt{235/f_y}$ and the plate non-dimensional slenderness as [17,18,25]:

$$\bar{\lambda}_p = \frac{b/t}{28.4\varepsilon\sqrt{k_\sigma}} \tag{13}$$

3. Numerical model

The finite element model used in this work was implemented using the software SAFIR, which has been developed specifically for the analysis of structures for the case of fire [26]. Geometric and material non-linear analysis with imperfections (GMNIA) using shell finite element models were carried out. The capability of SAFIR to model local buckling with shell elements was validated by Talamona and Franssen [27]. The beams were modelled using shell elements with four nodes and six degrees of freedom (3 translations and 3 rotations). These shell elements adopt the Kirchoff's theory formulation with a total co-rotational description. A study on the mesh sensitivity was performed and the solution converged for the members discretized with 100 divisions per 10.0 m on the length, 10 divisions on the flange width and 22 divisions on the web height, which was the mesh used in this study. The steel material model adopted a two-dimensional constitutive relation with the von Mises yield surface according to the non-linear stress–strain formulae of Eurocode 3 (see Fig. 1) and the respective reduction factors at elevated temperatures ($k_{y,\theta}$, $k_{p,\theta}$ and $k_{E,\theta}$). The integration of the shell elements was made with a Gauss scheme with 2×2 points on the surface and 4 points through the thickness. The temperature was considered uniform along the cross section and along the beam so that a comparison between the numerical results and the simple design equations is possible. Single span members with fork supports as boundary conditions were modelled. Vertical displacements (U_z) were prevented on both extremities of the beam on the lower flange (see Fig. 2), and lateral displacements (U_y) were also prevented in both extremities along the web, on one extremity. Displacements along the axis of the beam (U_x) were also blocked.

The loads were modelled by applying distributed forces (by means of nodal forces) on the flanges and on the web. The collapse load for the beam at elevated temperatures was determined by first increasing the temperature to the desired value and then applying an increasing load until failure was reached. The geometric imperfections were introduced in the model by changing the
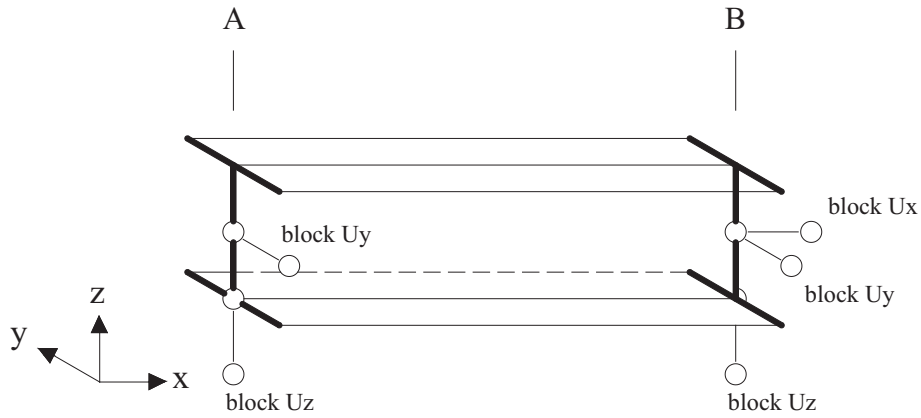
Fig. 2. Illustration of the boundary conditions in the numerical model.

node coordinates to represent the worst scenario for the assessment of lateral–torsional buckling resistance of the beams. The shape given by the eigenmodes of a linear buckling analysis performed with the software Cast3M [28] was used. In accordance with the recommendations for finite element method analysis given in Annex C of EN 1993-1-5 [25], a combination of global and local modes (see Fig. 3) was considered. Because slender cross sections were considered in this study, interaction between local buckling and lateral–torsional buckling was observed in the beam failures (see Section 5.1); thus, using a combination of modes led to lower resistance than considering only the lower mode. Accordingly, the combination of the modes was used with the lowest mode from the local or global considered as the leading imperfection and the other mode reduced to 70%. The amplitude of the imperfections was considered as 80% of the geometric fabrication tolerances given in the EN 1090-2 [29] as indicated in the same annex. That is, the global mode was scaled to 80% of $L/750$ and the local mode to 80% of $b/100$ or 80% of $h_w/100$, where b is the flange width and h_w is the height of the web of the cross section, depending on which node had the maximum displacement for the local mode. The recommendation in the standard to consider at least 4 mm as the geometric fabrication tolerances for the web was also taken into account.

Residual stresses were introduced in the numerical model with the stress pattern [30] depicted in Fig. 4. The values adopted for the residual stresses were according to [30,31], as used in a previous study [32].

As mentioned previously, the investigation of the ultimate capacity of laterally unrestrained beams with slender cross sections for the case of fire is very limited and experimental results are almost non-existent. In the scope of the European Research project FIDESC4 [33], three tests were performed on laterally unrestrained beams heated at elevated temperatures. The numerical model presented in this study was validated against those experimental tests and the results of this validation, as well as a mesh sensitivity study, are published in [34], showing good agreement between the numerical model and the experimental tests.

4. Comparison of FEA results to the actual beam design curve of Eurocode 3

In this section, a comparison is made between the numerical results obtained in SAFIR and the actual beam design curve from Part 1-2 of Eurocode 3 (see Section 2). Several slender cross sections with Class 3 and Class 4 classifications were considered in this study. The geometry of the cross sections are indicated in Table 1, along with the steel grade, temperatures and non-dimensional slenderness considered in the numerical study. Here, the cross-sectional resistance was calculated according to EN 1993-1-2, as given by Eq. (14) for Class 3 cross sections and Eq. (15) for Class 4 cross sections.

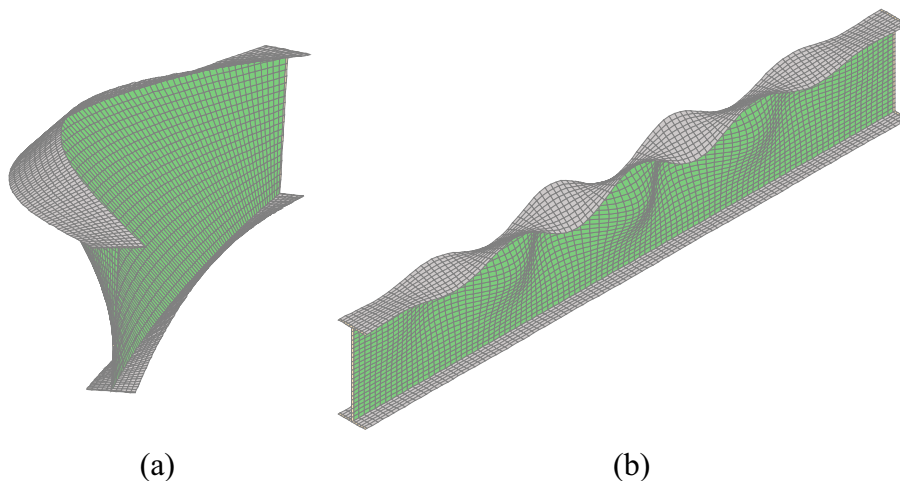$$M_{fi,Rd,EC3} = W_{el,y}k_{y,\theta}f_y/\gamma_{M,fi} \qquad (14)$$

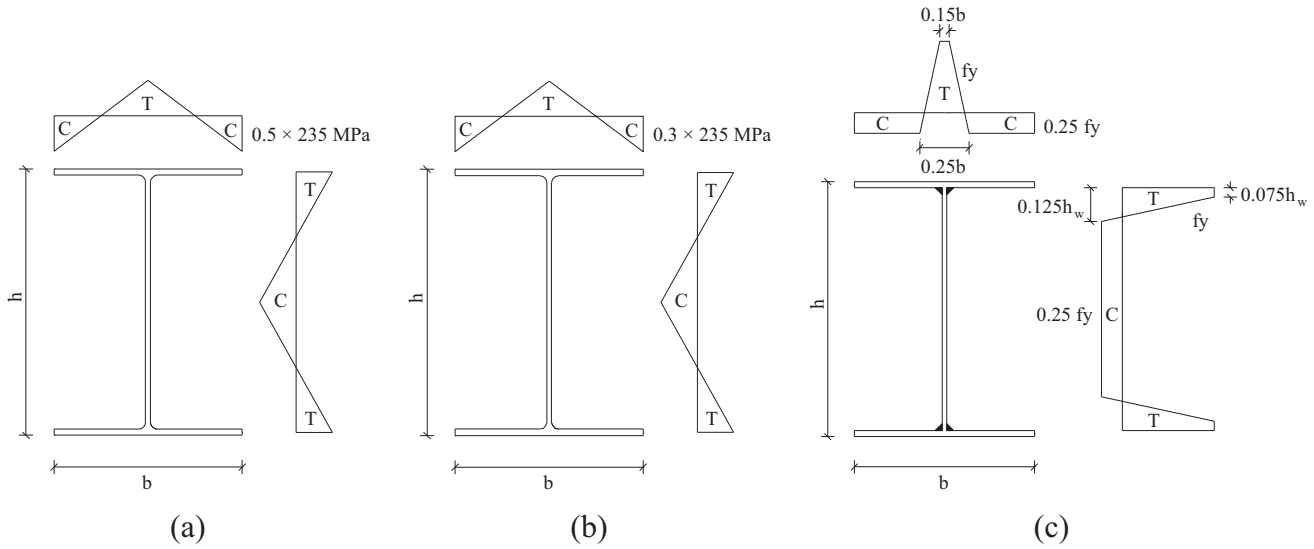**Fig. 3.** (a) Global eigenmode and (b) local eigenmode for introducing the imperfections.

Fig. 4. Pattern of the residual stresses considered in this study for (a) hot-rolled with $h/b \leqslant 1.2$, (b) hot-rolled with $h/b > 1.2$ and (c) welded profiles.

Table 1
Cases considered in the numerical study.

	Geometry $h_w \times t_w + b \times t_f$ (mm)	Flange thickness (t_f) (mm)	Steel grade	Temperatures	$\bar{\lambda}_{LT,\theta}$
	$450 \times 4 + 150 \times t_f$	5, 6, 7, 8, 9, 10, 11, 12, 13, 14, 15	S235, S275, S355 and S460	350 °C, 450 °C, 550 °C and 700 °C	[0, 2]
	$450 \times 4 + 200 \times t_f$	7, 8, 9, 10, 11, 12, 13, 14, 15, 16, 17, 18, 19, 20			
	$450 \times 4 + 250 \times t_f$	8, 10, 11.5, 13, 15, 16.5, 18, 20, 21.5, 23, 25			
	$450 \times 6 + 150 \times t_f$	8, 8.1, 8.2, 8.3, 8.4, 8.5, 9, 9.5, 10, 11.5, 13, 15, 16.5, 18, 20, 21.5, 23, 25			
	$450 \times 6 + 250 \times t_f$	13, 13.5, 14, 14.5, 15, 15.5, 16, 18, 20, 23, 25			
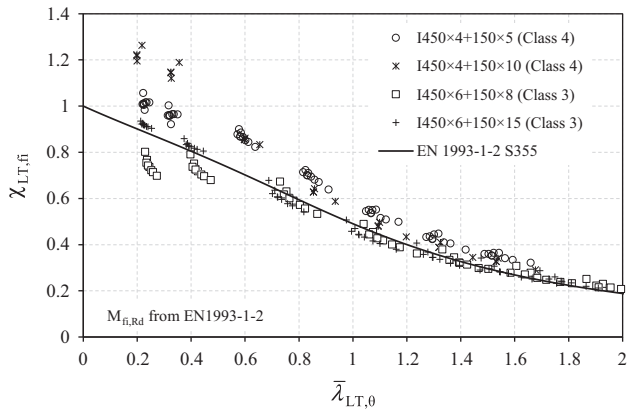
Fig. 5. Comparison of the actual LTB design curve of EN 1993-1-2 to the FEA simulations.

$$M_{fi,Rd,EC3} = W_{eff,y} k_{0.2p,\theta} f_y / \gamma_{M,fi} \quad (15)$$

For comparison purposes, Fig. 5 shows the results obtained with the FEA simulations carried out with SAFIR and the actual beam design curve from Part 1-2 of Eurocode 3 (EN 1993-1-2) for four cross sections representing different classifications cases for the steel grade S355 (see Table 2).

Fig. 5 shows distinct behaviour between Class 3 and Class 4 beams, particularly for low slenderness range $\bar{\lambda}_{LT,\theta} \approx 0.2$, where

Table 2
Geometry and classification of cross sections in fire.

	Dimensions ($h_w \times t_w + b \times t_f$) (mm)	Steel grade	Classification in fireweb – flange	Overall classification in fire
	$450 \times 6 + 150 \times 15$	S355	3 – 1	3
	$450 \times 4 + 150 \times 10$		4 – 3	4
	$450 \times 6 + 150 \times 8$		3 – 3	3
	$450 \times 4 + 150 \times 5$		4 – 4	4

the resistance of the beam is mainly governed by the cross section capacity.

For the beam with cross section I450 × 6 + 150 × 8 (web Class 3 and flange Class 3), the EN 1993-1-2 design curve over-predicts the beam capacity. For the cross section with a higher flange thickness (see I450 × 6 + 150 × 15, web Class 3 and flange Class 1), better agreement is achieved between the numerically predicted capacity and with EN 1993-1-2. For Class 4 beams, the actual design curve underestimates the beam capacity, especially for the Class 3 flange case (I450 × 4 + 150 × 10). This particular case of cross sections with a Class 4 web and a Class 3 flange is representative of the situations from which the designers may benefit more from using beams with slender cross sections. For the intermediate beams with $\bar{\lambda}_{LT,\theta} \approx 1.0$ and Class 3 cross sections, the curve is slightly unsafe.

Furthermore, in Fig. 6, the accuracy of EN 1993-1-2 is compared for all of the FEA simulations undertaken in this study, as indicated in Table 1.

The results obtained show the same pattern as that for the cases considered in Fig. 5 with distinct results obtained for Class 3 and Class 4 beams. Here, for non-dimensional slenderness values of $\bar{\lambda}_{LT,\theta} \approx 0.2$, more than 60% of the load bearing capacity is not considered for Class 4 beams, while for Class 3 beams, the EN 1993-1-2 curve over-predicts the capacity in more than 20%. On the subject of the resistance of slender cross sections for the case of fire, the authors have demonstrated in [16–18] that the cross-sectional resistance given by EN 1993-1-2 formulae in comparison to FEA for Class 3 and Class 4 is inadequate because it underestimates the resistance of Class 4 cross sections and overestimates the resistance of Class 3 cross sections.

Because the cross-sectional capacity influences the LTB resistance of the beams, the impact of using this new formulation should be studied. Thus, in Fig. 7, the results obtained with FEA and considering the cross-sectional resistance predicted by the FIDESC4 proposal, i.e., using Eq. (9), are shown for the previous four analysed cases. The results are less scattered compared to those obtained with the actual provisions for the cross-sectional resistance of EN 1993-1-2, given by Eqs. (14) and (15).

In Fig. 8, the FEA results are plotted against the EN 1993-1-2 design curve combined with the FIDESC4 proposal for the cross-sectional resistance.
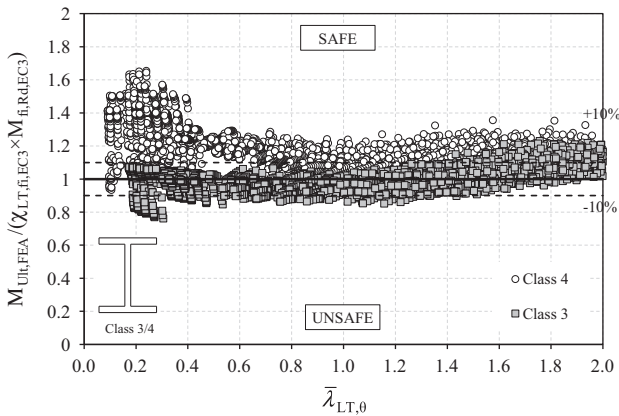
Fig. 6. Accuracy of the LTB design curve from EN 1993-1-2 compared to FEA results with cross-sectional resistance calculated according to EN 1993-1-2.
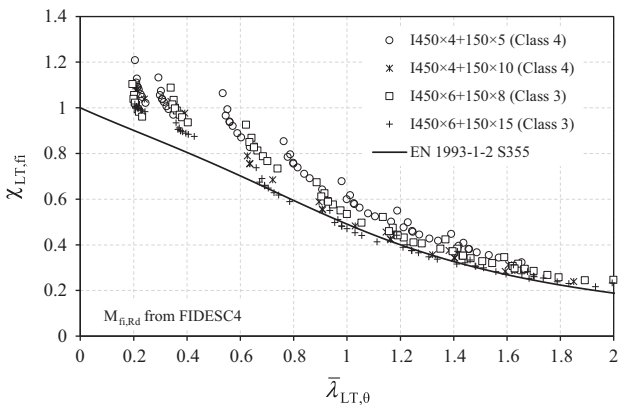
Fig. 7. Comparison of actual LTB design curve of EN 1993-1-2 with cross-sections calculated according to FIDESC4 (Eq. (9)) and FEA simulations.
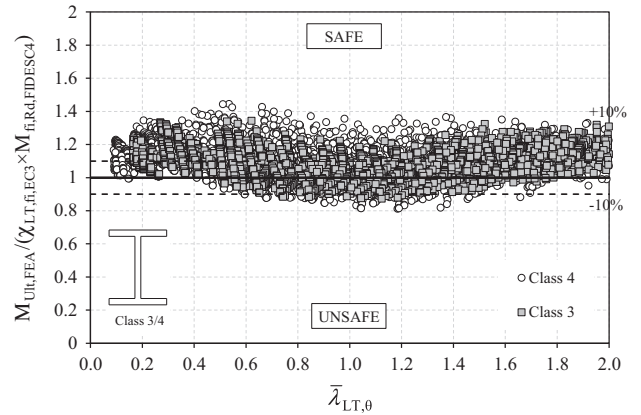
Fig. 8. Accuracy of the LTB design curve from EN 1993-1-2 compared to FEA results with cross-sectional resistance calculated according to the FIDESC4 proposal.

In this case, the deviation of the results is again smaller compared to Fig. 6, where the cross-sectional resistance was calculated according to EN 1993-1-2 provisions. For Class 3 beams, the results are now mainly on the safe side with a maximum of 10% on the unsafe side. For Class 4 beams, there is less load-bearing capacity disregarded moving from a maximum of 60% in Fig. 6 towards 40% in Fig. 8 for $\bar{\lambda}_{LT,\theta} \approx 0.2$. However, in the particular case of Class 4 cross sections, for $\bar{\lambda}_{LT,\theta} > 0.5$, the use of the FIDESC4 proposal for the cross-sectional resistance increased the scatter of the results compared to Fig. 6, ranging from −20% to almost 30% for instance for $\bar{\lambda}_{LT,\theta} \approx 1.0$. Although improvements are observed by considering the FIDESC4 proposal for the cross-sectional resistance, the actual LTB design curve of EN 1993-1-2, which was developed only for Class 1 and Class 2 beams [2,4], could be improved to better predict the capacity of beams with slender cross sections, as shown in the remaining part of this study. Nonetheless, for short members whereas the response of the beams is mainly influenced by the cross-sectional resistance, it was observed that a beneficial post-critical behaviour was obtained and for that reason the results in Fig. 7 are higher than 1.0 for low values of the non-dimensional slenderness. Although it is noteworthy, this phenomenon was not further studied because it is out of the scope of the present study.

Finally, it was observed that the Eurocode philosophy of decoupling local buckling from the lateral–torsional buckling by treating the first phenomenon using a reduced cross-sectional capacity and the latter with the appropriate reduction factor leads to inconsistent results. As demonstrated by different researchers [21–24], a coupled instability occurs in these cases and appropriate modifications to design rules should be investigated. A review, including the scientific background, for the coupled interaction that occurs for members with slender cross-sections is well described in [22] including a description for the local and lateral–torsional buckling interaction. The remaining part of this manuscript is dedicated to study numerically the influence of several parameters and propose improved design rules to account for that interaction for the case of fire.

5. Parametric study

To develop an improved design curve for beams with slender cross sections at elevated temperatures, a parametric study was performed to investigate the influence of various parameters using the numerical model described in Section 3. Here, only the uniform bending moment distribution was considered. First, the effective section factor concept is presented, and its influence on LTB

capacity is demonstrated; then, the influence of the temperature, the residual stresses, the steel grade and the depth-to-with ratio is also investigated.

5.1. The effective section factor concept and its influence

The load bearing capacity of beams with slender cross sections is influenced by the interaction between the resistance to local buckling of the cross section and the overall resistance of the beam to lateral–torsional buckling. To account for this interaction, it is here proposed to group the behaviour of the beams by considering an effective section factor s for the cross section given by:

$$s = W_{eff,y}/W_{el,y} \qquad (16)$$

where $W_{eff,y}$ is the effective section modulus and $W_{el,y}$ is the elastic section modulus, both for the strong axis. From the results, three different groups were identified according to the interaction between the local buckling and the lateral–torsional buckling as high ($W_{eff,y}/W_{el,y} \leqslant 0.8$), moderate ($0.8 < W_{eff,y}/W_{el,y} \leqslant 0.9$) or small ($W_{eff,y}/W_{el,y} > 0.9$). In Figs. 9–11, the numerical results are plotted for these ranges of effective section factor ratios. For ease of comparison, these figures also plot the EN 1993-1-2 design curve for steel grade S355 as a reference line.

These figures show different trends for the numerical results depending on the effective section factor, and the following conclusions can be highlighted:
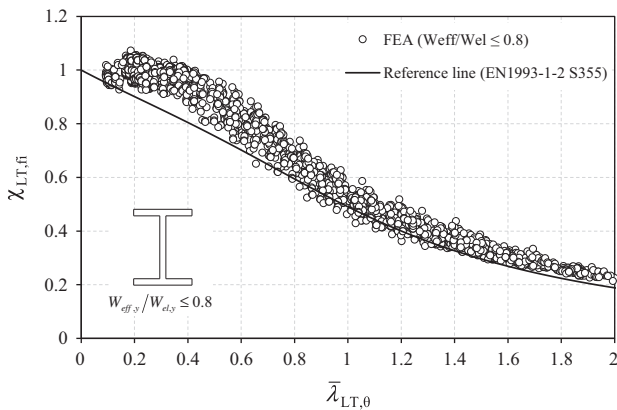
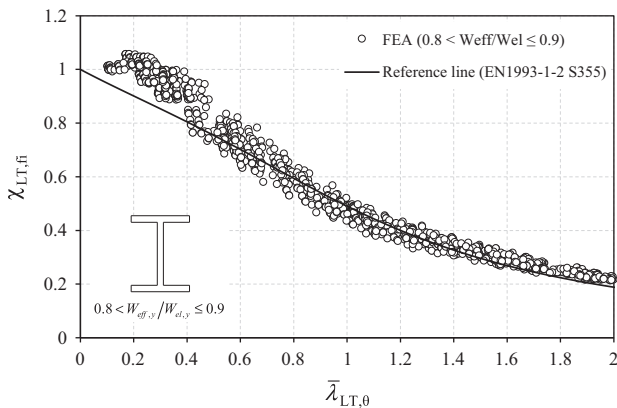**Fig. 9.** LTB behaviour of beams with an effective section factor of $W_{eff,y}/W_{el,y} \leqslant 0.8$.

Fig. 10. LTB behaviour of beams with an effective section factor of $0.8 < W_{eff,y}/W_{el,y} \leqslant 0.9$.
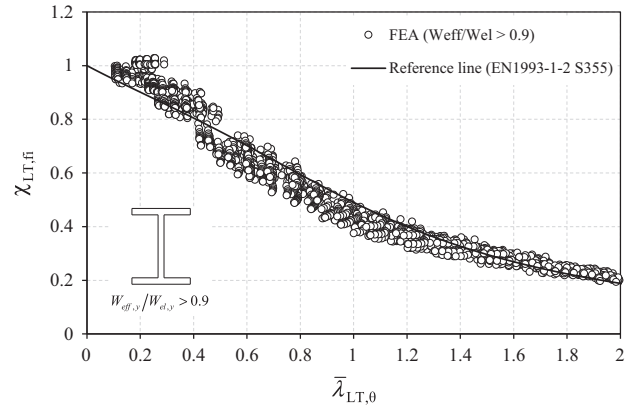

Fig. 11. LTB behaviour of beams with an effective section factor of $W_{eff,y}/W_{el,y} > 0.9$.

- $W_{eff,y}/W_{el,y} \leqslant 0.8$ plateaus until $\bar{\lambda}_{LT,\theta} \approx 0.4$, meaning that until this slenderness, the capacity of the beams is governed by the cross-sectional resistance. For higher slenderness ($\bar{\lambda}_{LT,\theta} > 0.4$), the capacity of the beam is reduced due to the interaction between the local buckling resistance of the cross section and the lateral–torsional buckling resistance of the member. However, in this effective section factor range, cross sections are more prone to local buckling, and therefore, its influence in the response of the beams is higher compared to the remaining ranges. For this purpose, the reduction of the overall load bearing capacity of the beams is also less in relative terms. For example, the minimum values of the reduction factor for a slenderness of $\bar{\lambda}_{LT,\theta} \approx 1.0$ in Fig. 9 is $\chi_{LT,fi} \approx 0.46$, in Fig. 10 is $\chi_{LT,fi} \approx 0.42$ and in Fig. 11 is $\chi_{LT,fi} \approx 0.37$, which represents a difference of approximately 10% in relative terms for each successive range.
- Compared to the previous case, the effective section factor of the cross section for $0.8 < W_{eff,y}/W_{el,y} \leqslant 0.9$, is higher, i.e., more effective, meaning that the cross section is less prone to local buckling, and therefore, the influence of local buckling in the overall response of the beams is less in relative terms. For this range, the plateau is smaller and placed at $\bar{\lambda}_{LT,\theta} \approx 0.3$. After this slenderness, the reduction of resistance is more severe due to the greater influence of the lateral–torsional instability mode compared to local buckling in the overall response of the beam.
- Finally, for $W_{eff,y}/W_{el,y} > 0.9$, the influence of the local buckling is even smaller compared to the previous cases, and consequently, the plateau is placed at $\bar{\lambda}_{LT,\theta} \approx 0.2$, and as expected, the reduction of the load bearing capacity is even more severe when compared to the previous ranges of effective section factor because it is mainly influenced by the lateral–torsional buckling resistance of the beam.
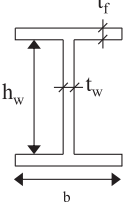
5.2. Temperature influence

The influence of temperature values on the lateral–torsional buckling resistance of laterally unrestrained beams was also analysed. The results obtained for the four sections described in Table 3 are detailed here. The steel grade considered was S355. The temperature distribution in the cross section and along the member was considered uniform so that comparison between the numerical results and simple design equations are possible. The temperature range of 350–700 °C (in 50 °C intervals) was used.

In Figs. 12–15, the results obtained for the various temperatures and for the cross sections indicated in Table 3 are shown.

From Figs. 12–15, LTB is not remarkably influenced by temperature. For this reason, the actual beam design curve of Part 1-2 of Eurocode 3 is not dependent on the temperature.

Table 3
Cross sections considered in the study of the influence of the temperature on the LTB resistance.

	Dimensions $(h_w \times t_w + b \times t_f)$ (mm)	Steel grade	Effective section factor $s = W_{eff,y}/W_{el,y}$
(I-section diagram with labels t_f, h_w, t_w, b)	$450 \times 6 + 150 \times 15$	S355	0.96
	$450 \times 4 + 150 \times 10$		0.85
	$450 \times 6 + 150 \times 8$		0.73
	$450 \times 4 + 150 \times 5$		0.60

Fig. 14. Influence of the temperature on the LTB resistance of the beams with a cross section of $450 \times 6 + 150 \times 8$ and effective section factor $W_{eff,y}/W_{el,y} = 0.73$.

Fig. 12. Influence of the temperature on the LTB resistance of beams with a cross section of $450 \times 6 + 150 \times 15$ and effective section factor $W_{eff,y}/W_{el,y} = 0.96$.

Fig. 15. Influence of the temperature on the LTB resistance of the beams with a cross section of $450 \times 4 + 150 \times 5$ and effective section factor $W_{eff,y}/W_{el,y} = 0.60$.

The residual stresses have an unfavourable influence on the LTB resistance of beams. In case of fire, this influence is less than that at normal temperature because in a fire, the temperature causes a relaxation of the residual stresses. Therefore, a maximum of a 15% reduction of the LTB resistance due to the residual stresses on beams with slender cross sections was observed for both hot-rolled and welded cases. The reduction of the LTB resistance is higher for intermediate slenderness values $1.0 \leqslant \bar{\lambda}_{LT,\theta} \leqslant 1.4$ for both cases, and for slenderness values of $\bar{\lambda}_{LT,\theta} \leqslant 0.4$, no influence was noticed of the residual stresses. Based on this comparison, the remainder of this study focuses only on the pattern corresponding to welded cross sections, as depicted in Fig. 4.

5.4. Steel grade influence

In this section, the influence of the steel grade is shown. Fig. 17a–d depicts the numerical results obtained for all of the profiles indicated in Table 1 with an effective section factor of $W_{eff,y}/W_{el,y} \leqslant 0.8$ and steel grades of S235, S275, S355 and S460, respectively; these steel grades have a yield strength at normal temperature of 235 MPa, 275 MPa, 355 MPa and 460 MPa, respectively. For the purpose of comparison, the EN 1993-1-2 design curves for each steel grade are plotted in all of the charts.

These figures show that the reduction of the beam capacity is dependent on the steel grade. The better the steel grade, the lower the reduction of the lateral–torsional buckling resistance of a beam. For example, for a slenderness of $\bar{\lambda}_{LT,\theta} \approx 1.0$, the minimum

Fig. 13. Influence of the temperature on the LTB resistance of the beams with a cross section of $450 \times 4 + 150 \times 10$ and effective section factor $W_{eff,y}/W_{el,y} = 0.85$.

5.3. Residual stresses influence

Here, the influence of residual stresses on the ultimate capacity of laterally unrestrained beams is investigated for the four different cross sections described in Table 3. Welded and hot-rolled cases are considered with the patterns of residual stresses defined in Fig. 4. The results are shown in Fig. 16 and are presented as the ratio between the ultimate load obtained in FEA with and without residual stresses. Various steel grades and temperatures (350 °C, 450 °C, 550 °C and 700 °C) were considered.
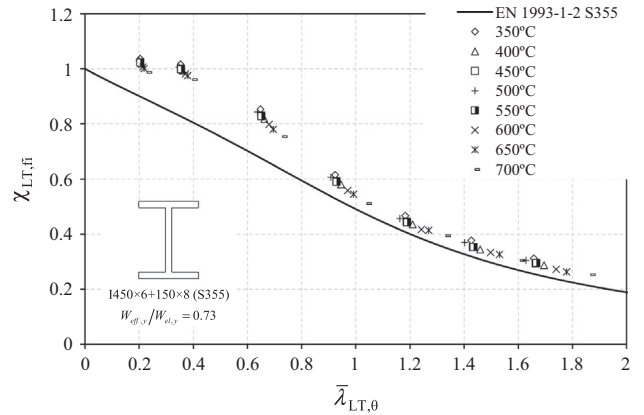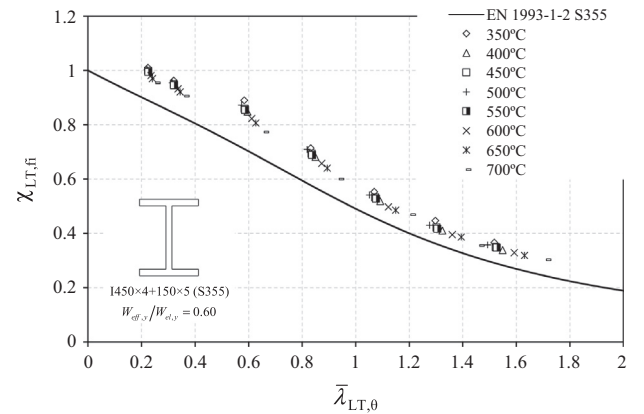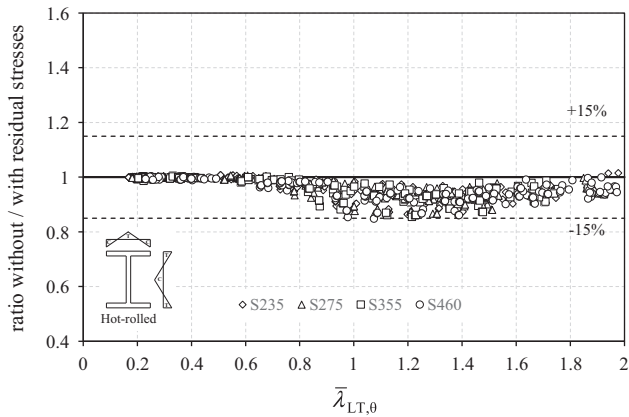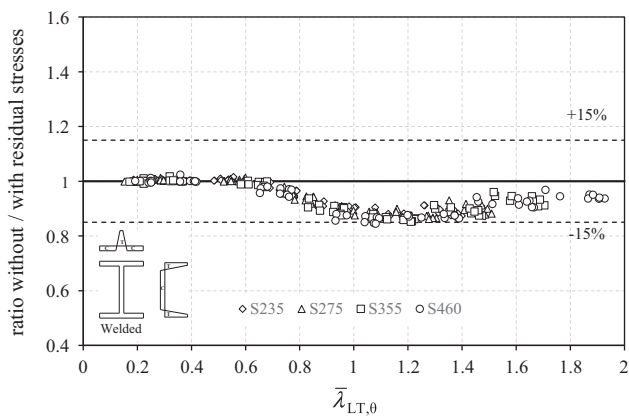
(a) Hot-rolled cross sections

(b)Welded cross sections

Fig. 16. Influence of the residual stresses on the LTB resistance of (a) hot-rolled and (b) welded beams with slender cross sections.

value for the reduction factor on the steel S235 is approximately $\chi_{LT,fi} \approx 0.46$ (see Fig. 17a), while for S460, it is approximately $\chi_{LT,fi} \approx 0.51$ (see Fig. 17d), which represents more than a 10% increase in resistance in relative terms. This is in line with the actual provisions of the Eurocode 3, which take the effect of steel grade into account in the verifications of beams against lateral–torsional buckling through the parameter α (see Eq. (4)). Although omitted here to save space, similar behaviour was obtained for other ranges of the effective section factor.
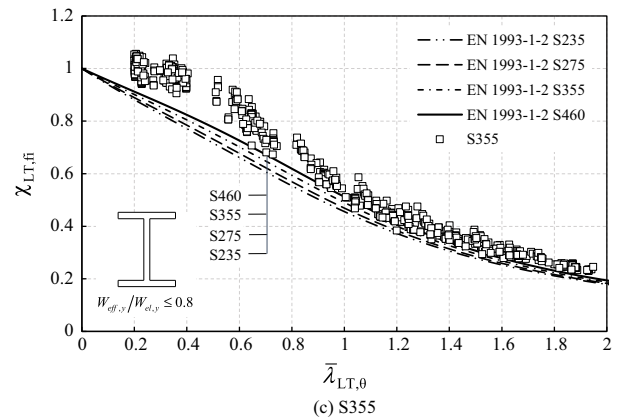
5.5. Depth-to-width ratio influence

The depth h to width b ratio (h/b) of a cross section is used in Part 1-1 of Eurocode 3 to group the properties of the sections and to take into account a variety of factors such as the torsional stiffness and the critical behaviour in plasticity, as noted in [35]. At elevated temperatures, this influence was also observed for Class 1 profiles in [8], and a severity factor that takes into account the influence of the h/b ratio among other parameters was suggested in that publication. In this section, the influence of the depth-to-width ratio is investigated for a variety of slender cross sections (see Table 1) considering different steel grades and temperatures (350 °C, 450 °C, 550 °C and 700 °C). Fig. 18 shows the influence of the depth-to-width ratio for an effective section factor of $W_{eff,y}/W_{el,y} \leqslant 0.8$ for steel grade S355.
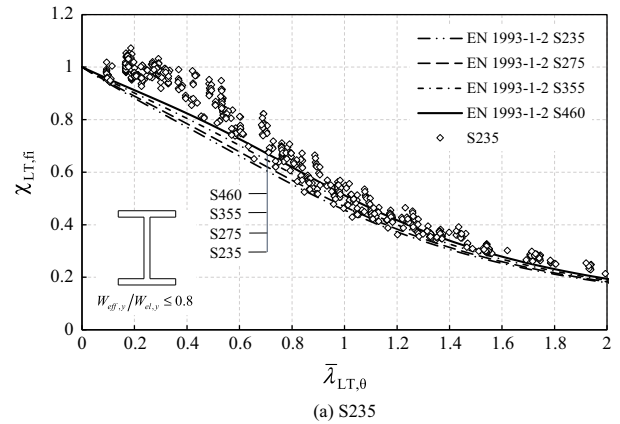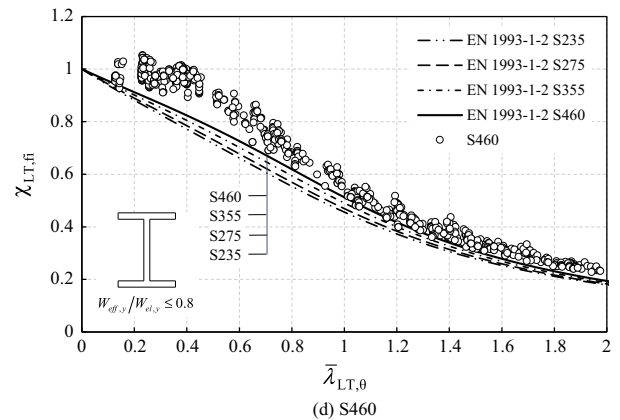

(a) S235
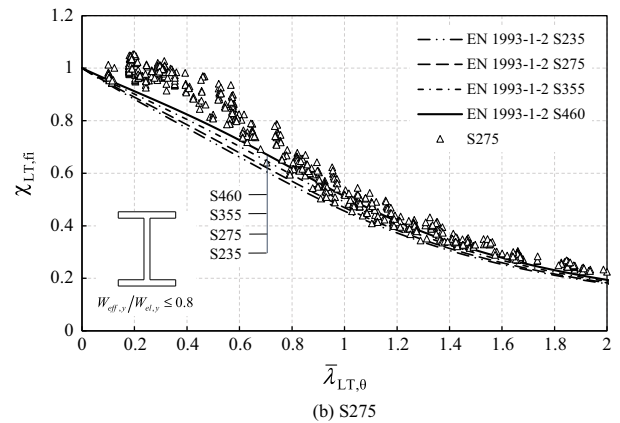
(b) S275

(c) S355

(d) S460

Fig. 17. LTB behaviour of beams with an effective section factor of $W_{eff,y}/W_{el,y} \leqslant 0.8$ for different steel grades.
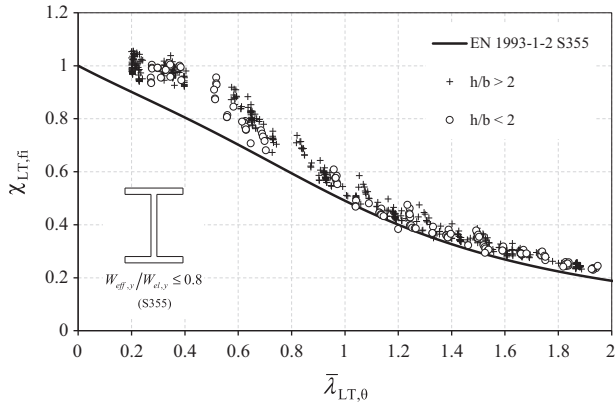
Fig. 18. Influence of the depth-to-width ratio on the LTB resistance of the beams for cross sections with $W_{eff,y}/W_{el,y} \leqslant 0.8$ and steel grade S355.

Fig. 19. New design curve for beams with slender cross sections at elevated temperatures (S235).

This figure shows that the influence of the depth-to-width ratio (h/b) is negligible for slender cross sections. As depicted in this figure, no distinct behaviour between sections with $h/b < 2$ and $h/b > 2$ is noticed. This parameter accounts for the critical behaviour in plasticity, and because slender cross sections are considered here, no differences in behaviour are observed. Although it is not demonstrated in this paper, similar trends were observed for other effective section factors and different steel grades.

6. New design curve

Based on the parametric study performed in Section 5, new design curves are proposed in this section. The improvements of using this new proposal compared to the design curve given in Part 1-2 of Eurocode 3 are also demonstrated here. The new design curves are dependent on the effective section factor (see Section 5.1) and on the steel grade (see Section 5.4), which are the main parameters that influence the lateral–torsional buckling behaviour of beams with slender cross sections at elevated temperatures. As stated previously, the influence of the steel grade was already taken into account in EN 1993-1-2 in the definition of the imperfection factor, using the parameter $\varepsilon = \sqrt{235/f_y}$ (see Eq. (5)). The proposed expressions are based on the actual design curve of Part 1-2 of the Eurocode, given by Eqs. (3)–(8), but also considering

$$\phi_{LT,\theta} = 0.5\left[1 + \alpha_{LT,new}(\bar{\lambda}_{LT,\theta} - \bar{\lambda}_{LT,0}) + \bar{\lambda}_{LT,\theta}^2\right] \quad (17)$$

with the values of $\alpha_{LT,new}$ and $\bar{\lambda}_{LT,0}$ given in Table 4. Three different curves are proposed (L1, L2 and L3) depending on the effective section factor. As observed in Section 5.1, plateaus ($\bar{\lambda}_{LT,0}$) of 0.4 and 0.3 would better represent the behaviour for the effective section factor $W_{eff,y}/W_{el,y} \leqslant 0.8$ and $0.8 < W_{eff,y}/W_{el,y} \leqslant 0.9$, respectively, but a constant plateau of 0.2 was adopted for all of the curves to simplify the proposal.

Fig. 20. Variation of the new design curve (L1) with the steel grade.

Fig. 21. Comparison between the new design curve for the beam with a cross section of $450 \times 6 + 150 \times 15$ and effective section factor $W_{eff,y}/W_{el,y} = 0.96$.

In Fig. 19, the proposed beam design curves L1, L2 and L3 are plotted for steel grade S235, and Fig. 20 depicts the variation of curve L1 with different steel grades.

A comparison between the numerical results obtained and the new design curve proposed in this work are shown in Figs. 21–24 for the cross sections indicated in Table 3.

Closer agreement is observed between the FEA numerical results and the proposed design curves (represented by the solid line in the figures). The introduction of the plateau $\bar{\lambda}_{LT,0} = 0.2$ improves the accuracy of the proposal for a small slenderness

Table 4
Parameters for the new design curve of beams with slender cross sections and criteria for selection.

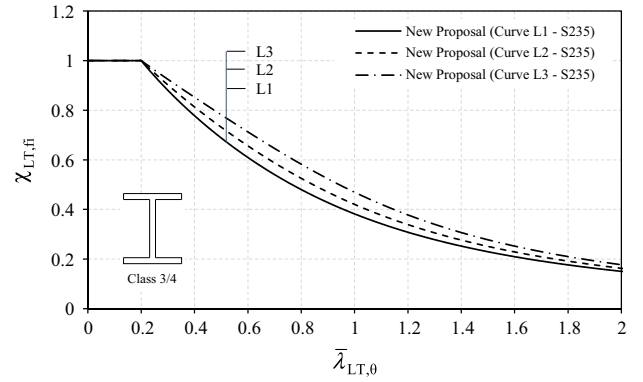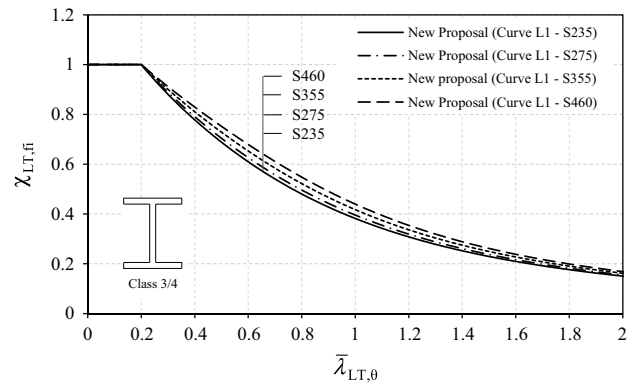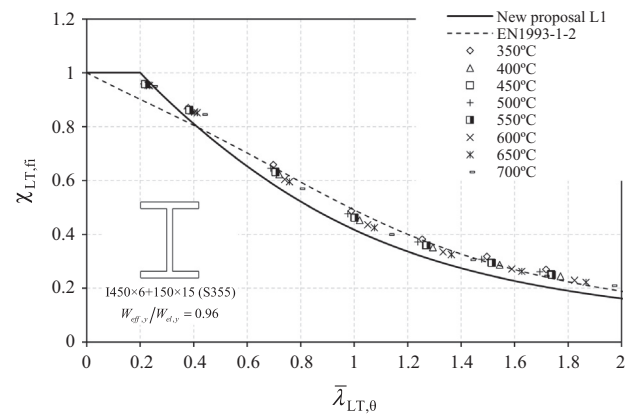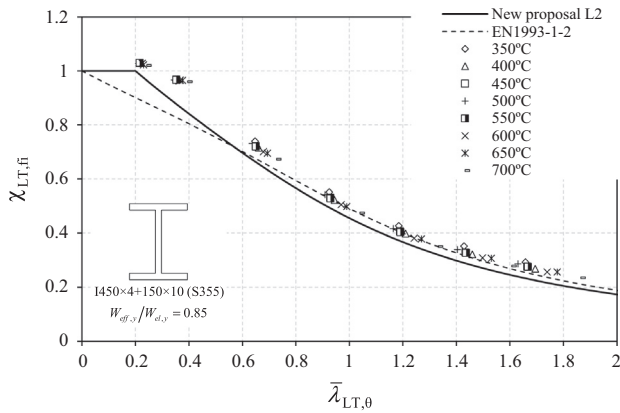| Curve	Limits	$\alpha_{LT,new}$	$\bar{\lambda}_{LT,0}$
L1	$\frac{W_{eff,y}}{W_{el,y}} > 0.9$	$1.25\varepsilon = 1.25\sqrt{235/f_y}$	0.2
L2	$0.8 < \frac{W_{eff,y}}{W_{el,y}} \leqslant 0.9$	$1.00\varepsilon = 1.00\sqrt{235/f_y}$	0.2
L3	$\frac{W_{eff,y}}{W_{el,y}} \leqslant 0.8$	$0.75\varepsilon = 0.75\sqrt{235/f_y}$	0.2

Fig. 22. Comparison between the new design curve for the beam with a cross section of 450 × 4 + 150 × 10 and effective section factor $W_{eff,y}/W_{el,y}$ = 0.85.

Fig. 23. Comparison between the new design curve for the beam with a cross section of 450 × 6 + 150 × 8 and effective section factor $W_{eff,y}/W_{el,y}$ = 0.73.

Fig. 24. Comparison between the new design curve for the beam with a cross section of 450 × 4 + 150 × 5 and effective section factor $W_{eff,y}/W_{el,y}$ = 0.60.

range $\bar{\lambda}_{LT,\theta} < 0.4$ when compared to EN 1993-1-2 (represented by the dashed line in the previous figures).

In practical terms, the proposed design curves should be used together with the cross-sectional resistance calculated according to FIDESC4 methodology (see Section 2.2); therefore, Fig. 25 presents its accuracy.
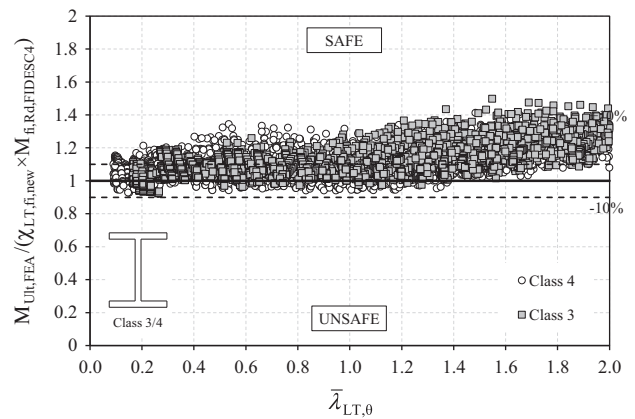

Fig. 25. Accuracy of the new design curve compared to FEA results with the cross-sectional resistance calculated according to the FIDESC4 proposal.
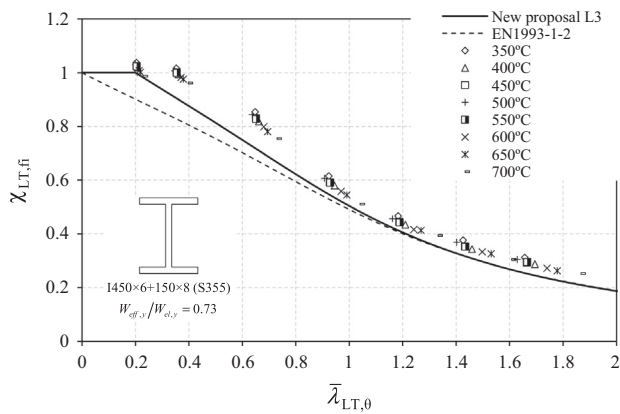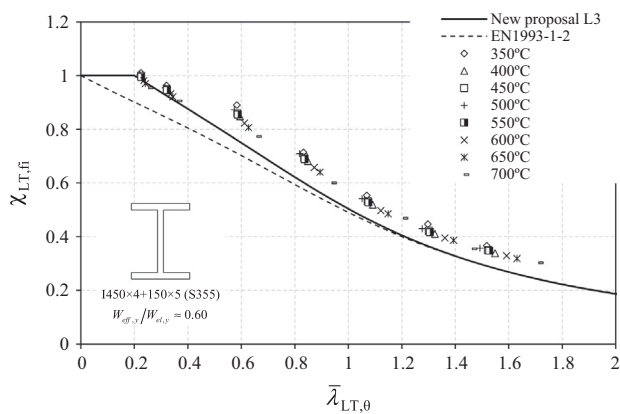
Figs. 25 and 8 are comparable, i.e., they show the new proposal and the EN 1993-1-2 design curve, respectively, considering the cross-sectional resistance calculated with the FIDESC4 proposal. The results are less scattered when using the proposed LTB design curves, especially for slenderness $\bar{\lambda}_{LT,\theta} \leqslant 1.0$, meaning that there is closer agreement between the numerical results and the proposal for the simplified design method. On the other hand, for slenderness around $\bar{\lambda}_{LT,\theta} \approx 1.0$, there are results that lay on the unsafe side for the EN 1993-1-2 design curve. As observed in Figs. 21 and 22, these are mainly Class 3 and Class 4 cross sections with an effective section factor tending towards unity and therefore less prone to local buckling. This problem can be corrected by considering curve L1, which is more conservative than the one in EN 1993-1-2. With the new proposal, the beam capacity is better predicted and the safety of using simplified design methods increases (going from a minimum of −20% for EN 1993-1-2 to −7% for the new proposal).

7. Conclusions

In this study, the behaviour of beams with slender cross sections subjected to uniform bending moment was investigated with finite element analysis software SAFIR for the case of fire. Shell finite elements were used, and several Class 3 and Class 4 cross sections as well as different temperatures and different steel grades were considered. In the first instance, the actual fire design rules of Part 1-2 of Eurocode 3 for checking the lateral–torsional buckling resistance of beams with slender cross sections could be improved. Using the current methodology to calculate the cross-sectional resistance at elevated temperatures to check the LTB resistance of beams for the case of fire, according to Part 1-2, leads to inaccurate results. The comparison to FEA carried out in SAFIR demonstrated that for small slenderness ranges of beams, the resistance was over-predicted for Class 3 cross sections and underestimated for Class 4 cross sections. A new methodology developed by the authors to calculate the cross-sectional capacity of Class 3 and Class 4 cross sections was then used to check the accuracy of the existing beam design rule, and improvements were observed. Nonetheless, the actual simplified methodology of EN 1993-1-2 could be improved to better account for the specific behaviour of beams with slender cross sections.

A parametric study was performed to investigate the influence of several parameters on the LTB resistance of beams with slender cross sections, namely, the effective cross section ratio $W_{eff,y}/W_{el,y}$, temperature, residual stresses, steel grade and depth-to-width ratio. From the studied parameters, the beam resistance depends on the effective ratio of the cross section. Therefore, an effective

section factor was proposed for this ratio $s = W_{eff,y}/W_{el,y}$, and different ranges were defined according to the influence of the local buckling on the lateral–torsional buckling resistance of beams: (i) for $W_{eff,y}/W_{el,y} \leqslant 0.8$ is high; (ii) For $0.8 < W_{eff,y}/W_{el,y} \leqslant 0.9$ is moderate and (iii) for $W_{eff,y}/W_{el,y} > 0.9$ is small.

Finally, a proposal for a new design curve including the effective section factor was proposed and validated against numerical results. The new proposal allows for better prediction of the capacity of beams with slender cross sections against lateral–torsional buckling for the case of fire.

Acknowledgements

References

[1] Bailey C, Burgess I, Plank R. The lateral-torsional buckling of unrestrained steel beams in fire. J Constr Steel 1996;36(2):101–19.
[2] Vila Real P, Franssen J-M. Numerical modeling of lateral-torsional buckling of steel I-Beams under fire conditions – Comparison with Eurocode 3. J Fire Prot Eng 2001.
[3] CEN. EN 1993-1-2, Eurocode 3: Design of steel structures – Part 1-2: General rules – structural fire design. Brussels: European Committee for Standardisation; 2005.
[4] Vila Real PMM, Piloto PAG, Franssen J-M. A new proposal of a simple model for the lateral-torsional buckling of unrestrained steel I-beams in case of fire: experimental and numerical validation. J Constr Steel Res 2003;59(2):179–99.
[5] Mesquita LMR, Piloto PAG, Vaz MAP, Vila Real PMM. Experimental and numerical research on the critical temperature of laterally unrestrained steel I beams. J Constr Steel Res 2005;61(10):1435–46.
[6] Vila Real PM, Lopes N, Simões da Silva L, Franssen J-M. Lateral-torsional buckling of unrestrained steel beams under fire conditions: improvement of EC3 proposal. Comput Struct 2004;82(20–21):1737–44.
[7] Vila Real PMM, Cazeli R, Simões da Silva L, Santiago A, Piloto P. The effect of residual stresses in the lateral-torsional buckling of steel I-beams at elevated temperature. J Constr Steel Res 2004;60(3–5):783–93.
[8] Vila Real PMM, Lopes N, Simões da Silva L, Franssen J-M. Parametric analysis of the lateral–torsional buckling resistance of steel beams in case of fire. Fire Saf J 2007;42(6–7):416–24.
[9] Dharma RB, Tan K-H. Proposed design methods for lateral torsional buckling of unrestrained steel beams in fire. J Constr Steel Res 2007;63(8):1066–76.
[10] Yin YZ, Wang YC. Numerical simulations of the effects of non-uniform temperature distributions on lateral torsional buckling resistance of steel I-beams. J Constr Steel Res 2003;59(8):1009–33.
[11] Zhang C, Gross JL, McAllister TP. Lateral torsional buckling of steel W-beams subjected to localized fires. J Constr Steel Res 2013;88:330–8.
[12] Lopes N, Vila Real PMM. Class 4 stainless steel I beams subjected to fire. Thin-Wall Struct 2014;83:137–46.
[13] CEN. EN 1993-1-1, Eurocode 3: Design of steel structures – Part 1-1: general rules and rules for buildings. Brussels: European Committee for Standardisation; 2005.
[14] Franssen J-M, Vila Real P. Fire design of steel structures. ECCS: Ernst & Sohn; 2010.
[15] Ranby A. Structural fire design of thin walled steel sections. J Constr Steel Res 1998;46(1–3):303–4.
[16] Couto C, Vila Real P, Lopes N, Zhao B. A new design method to take into account the local buckling of steel cross-sections at elevated temperatures. In: 8th International conference on structures in fire; 2014.
[17] Couto C, Vila Real P, Lopes N, Zhao B. Effective width method to account for the local buckling of steel thin plates at elevated temperatures. Thin-Wall Struct 2014;84:134–49.
[18] Couto C, Vila Real P, Lopes N, Zhao B. Resistance of steel cross-sections with local buckling at elevated temperatures. J Constr Steel Res 2015;109:101–14. http://dx.doi.org/10.1016/j.jcsr.2015.03.005.
[19] Schafer BW, Pekoz T. Direct strength prediction of cold-formed steel members using numerical elastic buckling solution. In: Shanmugam N, Liew JYR, Thevendran V, Shanmugam N, Liew JYR, Thevendran V, editors. Thin-Wall Struct – Res Dev (Ictws'98 Singapore, 2–4/12). Elsevier; 1998. p. 137–44.
[20] Schafer BW. Review: the direct strength method of cold-formed steel member design. J Constr Steel Res 2008;64(7–8):766–78.
[21] Dubina D. The ECBL approach for interactive buckling of thin-walled steel members. Steel Compos Struct 2001.
[22] Dubina D, Ungureanu V. Instability mode interaction: from Van Der Neut model to ECBL approach. Thin-Wall Struct 2013:1–11.
[23] Camotim D, Silvestre N, Basaglia C, Bebiano R. GBT-based buckling analysis of thin-walled members with non-standard support conditions. Thin-Wall Struct 2008;46(7–9):800–15.
[24] Camotim D, Basaglia C. On the behaviour, failure and direct strength design of thin-walled steel structural systems. Thin-Wall Struct 2014;81:50–66.
[25] CEN. EN 1993-1-5, Eurocode 3 – Design of steel structures – Part 1-5: plated structural elements. Brussels: European Committee for Standardisation; 2006. pp. 1–53.
[26] Franssen J-M. SAFIR, a thermal/structural program modelling structures under fire. Eng J AISC 2005;42(3):143–58.
[27] Talamona D, Franssen J-M. A quadrangular shell finite element for concrete and steel structures subjected to fire. J Fire Prot Eng 2005;15(4):237–64.
[28] CEA. CAST 3M is a research FEM environment; its development is sponsored by the French Atomic Energy Commission. <http://www-cast3m.cea.fr/>; 2012.
[29] CEN. EN 1090-2: execution of steel structures and aluminium structures – Part 2: technical requirements for steel structures. Brussels: European Committee for Standardisation; 2008.
[30] ECCS. Ultimate limit state calculation of sway frames with rigid joints. Publication No. 33. European Convention for Constructional Steelwork Technical Committee No. 8; 1984.
[31] ECCS. Manual on stability of steel structures. Publication No. 22. European Convention for Constructional Steelwork Technical Committee No. 8; 1976.
[32] ECCS. New lateral torsional buckling curves kLT – numerical simulations and design formulae. European Convention for Constructional Steelwork Technical Committee No. 8; 2000.
[33] FIDESC4. Fire design of steel members with welded or hot-rolled class 4 cross-section. RFCS-CT-2011-00030, 2011–2014. Technical Report No. 5; 2014.
[34] Prachar M, Lopes N, Couto C, Jandera M, Vila Real P, Wald F. Lateral torsional buckling of Class 4 steel plate girders under fire conditions: experimental and numerical comparison. In: Wald F CE, Burgess I, Kwasniewski L, Horová K, editors. Benchmark studies – experimental validation of numerical models in fire engineering. CTU Publishing House, Czech Technical University in Prague; 2014. p. 21–33.
[35] Taras A, Greiner R. New design curves for lateral–torsional buckling—proposal based on a consistent derivation. J Constr Steel Res 2010;66(5):648–63.